

# MoVieDrive: Multi-Modal Multi-View Urban Scene Video Generation

Guile Wu<sup>1</sup>, David Huang<sup>1,2\*</sup>, Dongfeng Bai<sup>1</sup>, and Bingbing Liu<sup>1</sup>

<sup>1</sup>Huawei Noah’s Ark Lab <sup>2</sup>University of Toronto

guile.wu@outlook.com, {baidongfeng, liu.bingbing}@huawei.com, dawae.huang@mail.utoronto.ca

## Abstract

Video generation has recently shown superiority in urban scene synthesis for autonomous driving. Existing video generation approaches to autonomous driving primarily focus on RGB video generation and lack the ability to support multi-modal video generation. However, multi-modal data, such as depth maps and semantic maps, are crucial for holistic urban scene understanding in autonomous driving. Although it is feasible to use multiple models to generate different modalities, this increases the difficulty of model deployment and does not leverage complementary cues for multi-modal data generation. To address this problem, in this work, we propose a novel multi-modal multi-view video generation approach to autonomous driving. Specifically, we construct a unified diffusion transformer model composed of modal-shared components and modal-specific components. Then, we leverage diverse conditioning inputs to encode controllable scene structure and content cues into the unified diffusion model for multi-modal multi-view video generation. In this way, our approach is capable of generating multi-modal multi-view driving scene videos in a unified framework. Our experiments on the challenging real-world autonomous driving dataset, nuScenes, show that our approach can generate multi-modal multi-view urban scene videos with high fidelity and controllability, surpassing the state-of-the-art methods.

## 1. Introduction

Urban scene video generation for autonomous driving has advanced rapidly in recent years. It can be used to generate controllable driving scenes, especially to synthesize long-tail scenarios that cannot be easily collected in real world. This facilitates performance enhancement and reliability evaluation in autonomous driving.

Contemporary video generation methods, such as SVD [2] and CogVideoX [38], have shown promising per-

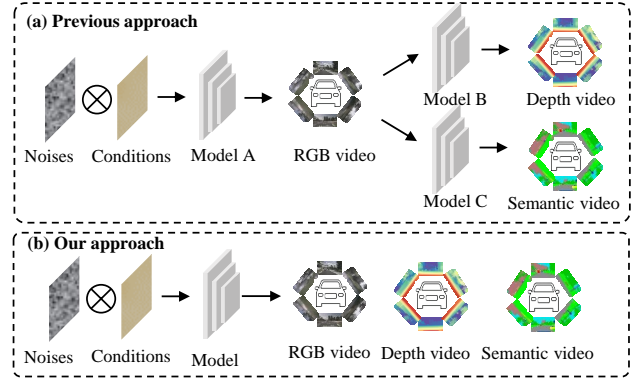


Figure 1. An illustration of different approaches to multi-modal multi-view driving scene generation. (a) Previous approaches typically require multiple models to generate different modalities, while (b) our approach employs a unified model for multi-modal multi-view joint generation.

formance for generating high-quality videos. However, they cannot be directly used for autonomous driving because multi-view driving scene generation requires multi-view spatiotemporal consistency and high controllability. To address this problem, some recent studies have explored diffusion models [10, 24] for controllable multi-view urban scene generation and shown promising performance [6, 21, 29, 33]. However, these methods mostly focus on single-modal RGB video generation and lack the ability to support multi-modal video generation. As a perception-intensive task, autonomous driving has an inherent need for multi-modal data, such as depth maps and semantic maps, which can facilitate holistic urban scene understanding towards safer and more efficient self-driving. A common approach to solving this problem is using multiple models to generate different modalities, but this often increases the difficulty of model deployment and does not fully exploit complementary cues for multi-modal data generation.

In this work, we propose a novel multi-**MO**dal multi-**VIEW** video diffusion approach, dubbed **MoVieDrive**, to autonomous driving. As illustrated in Fig. 1, instead of us-

\*D. Huang made contributions during an internship at Huawei.

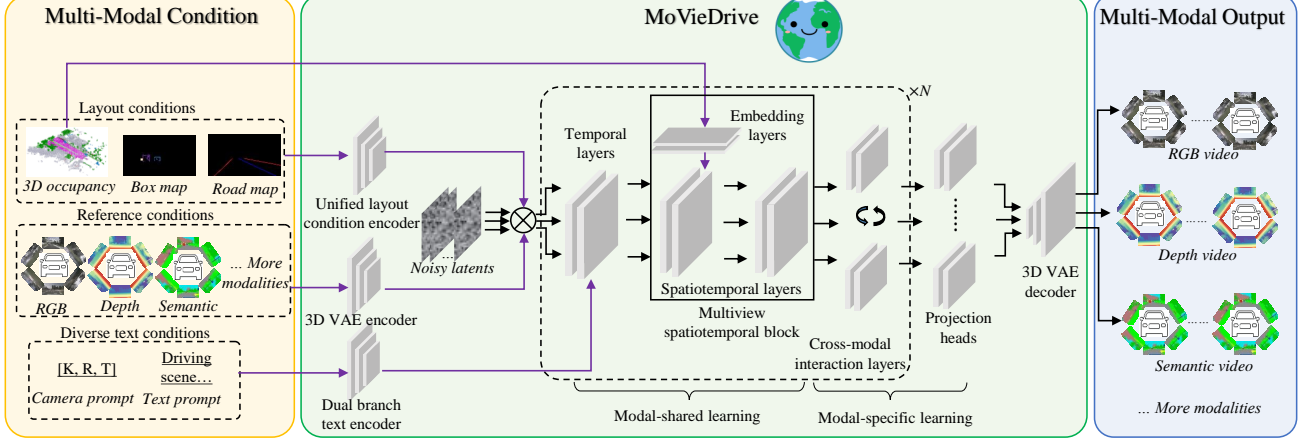


Figure 2. An overview of the proposed MoVieDrive approach. Our approach employs diverse conditioning inputs and a multi-modal multi-view diffusion transformer model to facilitate urban scene understanding in autonomous driving.

ing multiple models to generate different modalities, our approach proposes to employ a unified model for multi-modal multi-view driving scene generation. An overview of our approach is depicted in Fig. 2. Specifically, we employ diverse conditioning inputs, including text conditions, reference conditions, and layout conditions, to guide controllable scene generation. Among them, text conditions guide holistic scene generation, reference conditions are optional and only used for future scene prediction, and layout conditions capture fine-grained scene cues. Next, we decompose multi-modal multi-view scene generation into modal-shared learning and modal-specific learning, and devise a unified diffusion transformer model with modal-shared layers and modal-specific layers. This unified model alleviates the need for multiple models and improves model scalability. We then encode diverse conditions into the unified diffusion model for multi-modal multi-view scene generation. This helps to leverage complementary cues from multi-modal data for richer scene understanding to facilitate multi-modal multi-view urban scene generation in a unified framework. To evaluate the performance of our approach, we conduct extensive experiments on nuScenes [3], a challenging real-world autonomous driving dataset. Experimental results show that our approach achieves compelling video generation quality and controllability compared with the state-of-the-art methods, while supporting multi-modal data generation. In summary, our **contributions** are:

- We propose the first work that exploits diverse conditioning inputs and a diffusion transformer model for multi-modal multi-view autonomous driving scene generation. This resolves the limitation of existing works and facilitates urban scene understanding in autonomous driving.
- We devise a unified multi-modal multi-view diffusion

transformer model composed of modal-shared components and modal-specific components. This enables multi-modal multi-view urban scene generation in a unified model.

## 2. Related Work

**Video Generation.** As a long-standing research topic in computer vision, video generation has been well developed and various types of methods have been explored, *e.g.*, diffusion models [11], Variational Autoencoders (VAEs) [1], generative adversarial networks [27], autoregressive models [32], etc. Among them, diffusion-based methods [2, 11, 12, 38] have recently become predominant due to their superiority in controllability and fidelity. However, these methods cannot be directly applied to urban scene generation for autonomous driving, which requires multi-view spatiotemporal consistency and high controllability. To adapt them to complex controllable driving scene generation, substantial modifications are needed [7, 29]. Our approach shares the merits of diffusion-based video generation and devises a new multi-modal multi-view diffusion transformer model for autonomous driving.

**Urban Scene Synthesis.** The rapid advancement in urban scene and asset generation has significantly facilitated data synthesis and closed-loop evaluation in autonomous driving [7, 18, 37, 41]. There are two primary research directions in urban scene synthesis for autonomous driving. One line of work explores rendering methods, such as neural radiance fields and 3D Gaussian splatting, for urban scene synthesis [23, 34, 37, 41]. Despite high-fidelity scene synthesis, this type of method has poor controllability and diversity. Another line of work explores video generation, such as diffusion models [2, 38], for urban scene

generation [29, 33]. Among them, some studies focus on single-view generation [8, 30], while the others investigate multi-view generation [7, 21, 31]. Our work focuses on the more challenging multi-view setting. Diffusion models are widely used as the backbone for contemporary multi-view urban scene generation, such as DriveDreamer [29], Panacea [33], MagicDrive [7], MagicDrive-V2 [6], Drive-WM [31], MaskGWM [21], etc. Although these methods have shown promising results, they only focus on single-modal RGB video generation and lack the ability to generate multi-modal data for holistic scene understanding. In addition, UniScene [13] proposes using multiple models to generate RGB videos and LiDAR point clouds, but still fails to construct a unified model for multi-view multi-modal driving scene generation. Different from existing works, our approach proposes to generate multi-modal multi-view driving scene videos in a unified framework, which fills a gap left by existing methods.

**Multi-Modal Synthesis.** There have been some diffusion-based multi-modal synthesis methods proposed in recent years [17, 26, 35, 39]. However, none of them are designed for urban scene generation and modifying them for complex controllable multi-modal multi-view scene generation is not trivial. Our approach differs from these works in that we propose a novel framework that uses diverse conditioning inputs to encode controllable scene structure and content cues into a diffusion transformer model for multi-modal multi-view driving scene generation.

### 3. Methodology

#### 3.1. Approach Overview

**Problem Statement.** This work focuses on multi-modal multi-view urban scene video generation for autonomous driving. Specifically, our goal is to learn a model conditioned on scene descriptions, *e.g.*, text prompts, box maps, etc., to generate scene videos for  $M$  modalities, *e.g.*, RGB videos, depth map videos, semantic map videos, etc. Each scene video consists of  $K$  frames and  $V$  camera views.

**Pipeline Overview.** Fig. 2 depicts an overview of our approach. Our approach follows the paradigm of diffusion-based video generation [6, 29]. As shown in the left of Fig. 2, we construct the scene descriptions with text conditions, reference conditions, and layout conditions, and employ the corresponding encoders to extract the embeddings of these conditions. The embeddings of layout conditions and reference conditions are concatenated with noisy latents  $x$  as inputs  $z$  to a diffusion model, while the embeddings of text conditions are injected into the diffusion model through cross-attention layers. Here, noisy latents

$x$  are obtained by sampling random noises from the Gaussian distribution during inference and by adding scheduled noises to the groundtruth frame latents extracted by a VAE encoder during training. Next, as shown in the middle of Fig. 2, we construct a multi-modal multi-view diffusion transformer model with modal-shared layers, composed of temporal layers and multi-view spatiotemporal blocks, and modal-specific layers, composed of cross-modal interaction layers and projection layers. We then train the diffusion transformer model to estimate the added noises  $\epsilon \sim \mathcal{N}(0, I)$  from the conditioned inputs  $z$ , so as to generate clean latents  $x'$  for each modality. Finally, as shown in the right of Fig. 2, the clean latents  $x'$  are used as inputs to a VAE decoder to produce multi-view scene videos for each modality. In the following sections, we present the details of conditioning inputs encoding, multi-modal multi-view diffusion transformer, and model training and inference.

#### 3.2. Conditioning Inputs Encoding

**Text Conditions.** Following [6, 29], text conditions are used to guide holistic scene generation. In our framework, we employ two types of text conditions, including camera prompts and text prompts, and use dual text encoders to generate text condition embeddings  $f^{text}$ . For camera prompts  $c^{cam}$ , we concatenate the camera intrinsic and extrinsic parameters applied with the Fourier embedding [19] and employ an MLP-based encoder  $E^{cam}$  to extract camera embeddings. For text prompts  $c^{text}$ , we use video caption descriptions and apply a frozen T-5 text encoder [22]  $E^{text}$  to extract text embeddings. We concatenate these embeddings as  $f^{text}$ . This process can be formulated as:

$$f^{text} = E^{cam}(c^{cam}) \otimes E^{text}(c^{text}), \quad (1)$$

where  $\otimes$  denotes concatenation.

**Layout Conditions.** For fine-grained scene structure and content control, we employ three types of layout conditions, including box maps, road maps and occupancy-based layout maps. These layout conditions can be obtained from human annotations or pretrained models and are useful to control fine-grained details in complex multi-view driving scene generation. For box maps, different from [6, 7] which uses box coordinates to extract box embeddings, we directly generate 2D box maps  $c^b$  by projecting target 3D box locations onto image planes and assign different colors to different categories. For road maps  $c^r$ , we project road structure cues (lane dividers, pedestrian crossings and lane boundaries) onto image planes and assign different colors to different categories. In addition, following [14], we use occupancy-based layout maps  $c^o$  to further enhance scene fine-grained control. This is accomplished by projecting sparse 3D occupancy onto an image plane to generate sparse semantic maps. Note that these semantic maps are coarse and sparse,

which are different from the dense semantic modality used for urban scene understanding in autonomous driving. 3D occupancy has been well explored in autonomous driving, and in practice, 3D occupancy can be obtained from an off-the-shelf model [13] or a simulator [5].

To encode these layout conditions, unlike prior work [6, 7, 29, 40] which employs multiple encoders, we propose to use a unified layout encoder to fuse these conditions before feeding them to the diffusion model. Specifically, we employ causal convolutional layers to construct causal resnet blocks inspired by [38]. We then construct the unified layout encoder with separate causal blocks for each condition and a shared causal resnet block for all conditions. In this way, we fuse layout conditions to generate layout condition embeddings  $f^{layout}$  for controllable scene generation. This can be formulated as:

$$f^{layout} = E_s^l(E_b^l(c^b) \otimes E_r^l(c^r) \otimes E_o^l(c^o)), \quad (2)$$

where  $E_b^l$ ,  $E_r^l$  and  $E_o^l$  are causal resnet blocks for processing each condition, while  $E_s^l$  is the shared causal resnet block.

**Reference Conditions.** In urban scene generation, reference conditions  $c^{ref}$  refer to the initial frame conditions which are optional and only used for future scene prediction similar to world models [21, 29]. We employ a 3D VAE encoder  $E^{vae}$  [38] to encode these reference conditions but set the temporal dimension to 1 since each modality usually has only one initial frame. Note that in our approach, we employ a shared pre-trained 3D VAE from CogVideoX [38] for all modalities, rather than using different VAEs for different modalities. Since the 3D VAE in CogVideoX [38] is trained with a massive corpus of real-world videos, it performs well for encoding and decoding videos of different modalities. During model training, we use the shared pre-trained 3D VAE encoder to extract groundtruth frames latents to generate noisy latents. Therefore, the conditioned inputs  $z$  is obtained by:

$$z = E^c(f^{layout} \otimes E^{vae}(c^{ref})) \otimes x, \quad (3)$$

where  $E^c$  is a convolutional layer to modulate the embedding dimension to be the same as  $x$ .

### 3.3. Multi-Modal Multi-View Diffusion Transformer

Contemporary video diffusion models cannot be directly used for multi-view controllable urban scene generation. On the other hand, existing driving video diffusion models lack the ability to generate multi-modal data for holistic scene understanding. To resolve this problem, we devise a new multi-modal multi-view diffusion transformer model in this work.

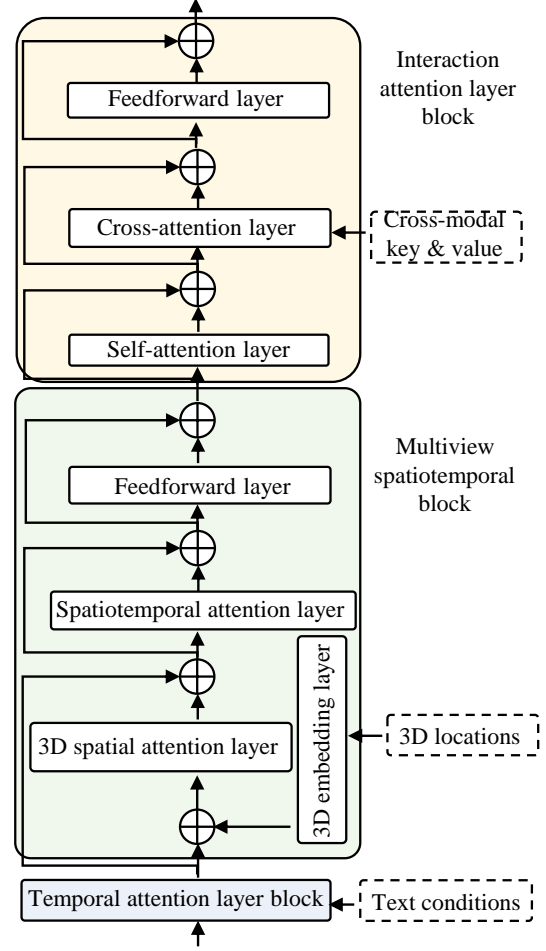


Figure 3. An illustration of the proposed diffusion transformer block. Here, adaptive normalization, scaling and shifting are used between each layers to modulate latents.

Specifically, since a shared pre-trained 3D VAE  $E^{vae}$  can be used to encode and decode videos of different modalities, we conjecture that *different modalities share a common latent space* and only require certain components to capture modal-specific content in order to distinguish them. In light of this, we decompose the model learning process into modal-shared learning and modal-specific learning and construct a unified diffusion transformer model with modal-shared components and modal-specific components.

For modal-shared components, we use temporal attention layers  $D^{tem}$  with 3D full attention from CogVideoX [38] to learn temporal consistency across video frames and inject text conditions  $f^{text}$  through cross-attention in the temporal attention layers. Here, the dimension of conditioned inputs  $z$  of each modality is transformed from  $\mathcal{R}^{V \times K \times H \times W \times C}$  to  $\mathcal{R}^{V \times (NKW) \times C}$  for the temporal attention layers. However, these temporal layers cannot guarantee spatiotemporal consistency for multi-view video



generation. Hence, we append multi-view spatiotemporal blocks  $D^{st}$  after temporal layers blocks to learn scene structure and capture spatiotemporal consistency. As shown in Fig. 3, each multi-view spatiotemporal block consists of a 3D spatial attention layer, a 3D spatial embedding layer, a spatiotemporal attention layer and a feedforward layer. The 3D spatial embedding layer is a multi-resolutional Hash grid [20] that encodes 3D occupancy locations  $c^{occ}$  into 3D spatial embeddings, which are added to latents from the temporal layers block to enhance spatial consistency. The 3D spatial attention layer is a self-attention layer that transforms the latent dimension to  $\mathcal{R}^{K \times (VHW) \times C}$  to learn 3D spatial structure information of all surrounding camera views. The spatiotemporal attention layer is a 3D full attention layer that transforms the latent dimension to  $\mathcal{R}^{(VKHW) \times C}$  to capture full spatiotemporal information for multi-view driving scene generation. In practice, we append the multi-view spatiotemporal block after every  $\alpha_1$  temporal layers block rather than every block. The feedforward layer is a fully-connected layer used to further transform latents. Note that following [38], we also employ adaptive normalization between each layer and adaptive scaling and shifting to modulate latents. We define this process as:

$$h = D^{st}(D^{tem}(z', f^{text}, t), c^{occ}, t), \quad (4)$$

where  $t$  is the diffusion timestep,  $z'$  is the latents output from the previous layers, and  $h$  is the latents output from the modal-shared layers.

For modal-specific components, we construct each cross-modal interaction layer block  $D_m^{cm}$  with a self-attention layer, a cross-attention layer, and a feedforward layer, where adaptive normalization between each layer and scaling and shifting are also used. Here, the query of the cross-attention layer is the latents of each modality, while the key and the value are from the concatenated latents of the other modalities. This cross-modal interaction layer block is used to learn modal-specific content while maintaining cross-modal alignment. In practice, the cross-modal interaction layer block is appended after every  $\alpha_2$  modal-shared layers. For each modality, this can process is formulated as:

$$h'_m = D_m^{cm}(h, h_m^{modal}, t), \quad (5)$$

where  $h'_m$  is the modal-specific latents output from the cross-modal interaction layer,  $h_m^{modal}$  denotes the key and the value from other modalities for the cross-attention layer. After  $N$  modal-shared layers and cross-modal interaction layers, we employ the modal-specific projection head (a linear layer with adaptive normalization) to estimate the added noises  $\epsilon$  and generate the clean latents  $x'$  for each modality. The clean latents  $x'$  for each modality is used as the input to a VAE decoder [38] to generate modal-specific multi-view

scene videos. In this way, our diffusion transformer model is capable of generating multi-modal multi-view videos with high fidelity, controllability and spatiotemporal consistency, in a unified framework. Note that our approach can be used for both one-modal and multi-modal generation, and the modalities are not limited to RGB videos, depth maps, and semantic maps, but can be extended to other modalities, *e.g.*, normal maps, flow maps, etc.

### 3.4. Model Training and Inference

For model training, we employ the DDPM [10] noise scheduler and define the training objective  $\mathcal{L}$  for multi-modal generation as:

$$\mathcal{L} = \sum_m^M \lambda_m \mathbb{E}_{x_{0,m}, t_m, \epsilon_m, C} \|\epsilon_m - \epsilon_{\theta, m}(x_{t,m}, t_m, C)\|^2, \quad (6)$$

where for the  $m$ th modality,  $\lambda_m$  is the weight for the training loss,  $x_{0,m}$  is the groundtruth clean latent,  $x_{t,m}$  is the noisy latent,  $C$  is the condition,  $\epsilon_{\theta, m}$  is the diffusion model,  $t_m$  is the timestep. Besides, conditioning dropout is used as an augmentation strategy to improve model generalization and output diversity. During inference, random noises are sampled from the Gaussian distribution as the model inputs. We employ the DDIM [25] sampler to improve the efficiency of the reverse diffusion process and classifier-free guidance (CFG) [9] to balance output diversity and condition consistency.

## 4. Experiments

### 4.1. Dataset and Experimental Setup

**Dataset.** Following previous works [6, 7, 29], we conduct experiments on the challenging nuScenes [3] dataset. The nuScenes dataset is a real-world autonomous driving benchmark, containing 700 training videos and 150 validation videos. We use the official training and validation splits for experiments. For layout condition, we extract road maps and box maps following [7, 29] and prepare 3D occupancies following [14]. For reference conditions, we employ the first frames of all camera views following the common practice [29]. For text conditions, we utilize the camera intrinsic and extrinsic parameters as the camera prompt and prepare text prompts using CogVLM2-Caption [38]. For multi-modal training data preparation, we employ RGB videos from the official dataset and generate depth maps with Depth-Anything-V2 [36] and semantic maps with Mask2Former [4]. Note that other off-the-shelf models can also be used to prepare multi-modal training data. Since the goal of this work is not to surpass the state-of-the-art depth or semantic models but to demonstrate multi-modal multi-view scene generation in a unified model, we leave the integration of more state-of-the-art models for future work.

Method	Video Fidelity	Scene Controllability		Depth Quality		Semantic Quality	
	FVD↓	mAP↑	mIoU↑	FVD↓	AbsRel↓	FVD↓	mIoU↑
DriveDreamer	340.8	-	-	-	-	-	-
DrivingDiffusion	332.0	-	-	-	-	-	-
Drive-WM	122.7	-	-	-	-	-	-
Panacea	139.0	-	-	-	-	-	-
MagicDrive	217.9	11.5	18.3	84.4	0.255	72.8	23.5
DriveDreamer-2	55.7	-	-	-	-	-	-
UniScene	70.5	-	-	-	-	-	-
MaskGWM	65.4	-	-	-	-	-	-
MagicDrive-V2	94.8	18.2	20.4	130.1	0.280	76.2	22.4
CogVideoX + SyntheOcc	60.4	15.9	28.2	51.6	0.124	298.9	32.4
Ours	<b>46.8</b>	<b>22.7</b>	<b>35.8</b>	<b>25.3</b>	<b>0.110</b>	<b>36.2</b>	<b>37.5</b>

Table 1. Quantitative comparison with the state-of-the-arts on nuScenes. Some results are cited from the original papers.



Figure 4. Qualitative comparison with the state-of-the-art methods. From left to right, we show results of back-right, back, back-left, front-left, front and front-right cameras and highlight some noticeable details.

**Evaluation Metrics.** For video fidelity evaluation, we use the commonly used Fréchet Video Distance (FVD) [28] as the metric. To evaluate the controllability, following [6], we use the pre-trained BEVFormer [16] to evaluate video-based 3D object detection in terms of mAP and video-based BEV segmentation in terms of mIoU. To evaluate the quality of the generated depth maps, we also use the Absolute Relative Error (AbsRel) [36]. Additionally, to evaluate the quality of generated semantic maps, we report mIoU for traffic-related classes, buildings, trees, and sky.

**Implementation Details.** We build our model on CogVideoX(v1.1-2B) [38] and SyntheOcc [14]. We employ the pre-trained T5 text encoder [22] and initialize the 3D

VAE and the temporal layers with the pre-trained weights from [38]. During training, the 3D VAE and the T5 text encoder are frozen, while the other model components are jointly trained. Our model is trained using the AdamW optimizer with a learning rate of  $2e^{-4}$ . By default, we use 6 cameras and 49 video frames, each with a resolution of  $512 \times 256$ .

## 4.2. Comparison with the State-of-the-Arts

**Compared Methods.** We compare our approach with several state-of-the-art urban scene video generation methods, including MagicDrive [7], MagicDrive-V2 [6], DriveDreamer [29], DriveDreamer-2 [40], Drive-WM [31], Panacea [33], UniScene [13], MaskGWM [21], and Driv-

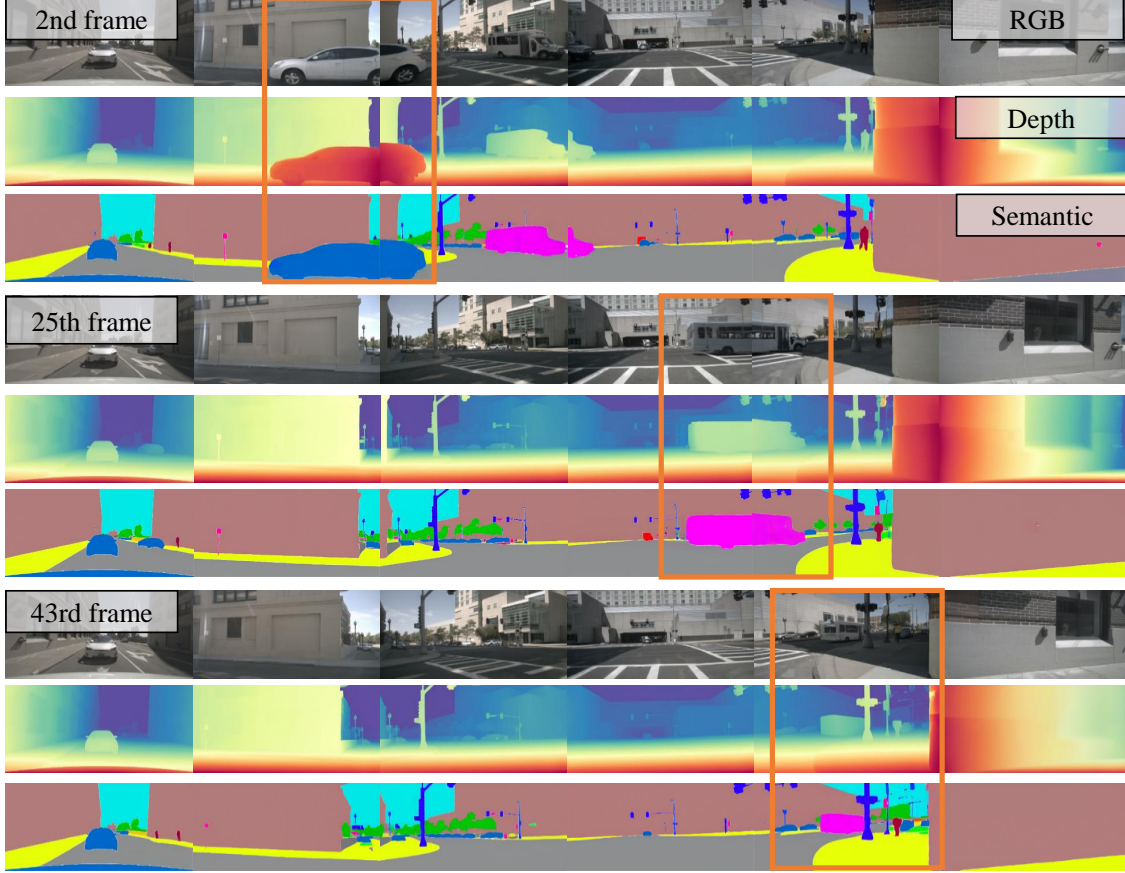


Figure 5. Visualization of cross-modal consistency.

ingDiffusion [15]. Besides, since we build our model on CogVideoX [38] and SyntheOcc [14], we use CogVideoX + SyntheOcc for multi-view scene video generation and consider it as our direct competitor. Moreover, since existing driving scene video generation methods lack the multi-modal generation capability, we use Depth-Anything-V2 and Mask2Former to estimate their depth maps and semantic maps. Note that single-view methods, such as Vista [8], are not our direct competitors because they cannot be directly used for multi-view video generation.

**Result Analysis of Video Fidelity.** Video fidelity measures the realism and temporal coherence of generated urban scene videos. We report FVD results in Tab. 1 and show that our approach achieves better results compared with the state-of-the-art methods. Specifically, our approach achieves FVD of 46.8, which is better than the state-of-the-art DriveDreamer, DriveDreamer-2, UniScene, MaskGWM, MagicDrive, etc. Besides, compared with CogVideoX + SyntheOcc, our approach improves performance by around 22%. Fig. 4 shows some qualitative comparison with the state-of-the-art methods. From Fig. 4, we

can see that our approach can produce urban scene videos with high-fidelity details, *e.g.*, vehicles and road structures.

**Result Analysis of Scene Controllability.** Scene controllability refers to the consistency between the conditioning inputs and the generated videos. We report mAP for 3D object detection and mIoU for BEV segmentation in Tab. 1. We can see that our approach achieves the best mAP of 22.7 for 3D object detection and the best mIoU of 35.8 for BEV segmentation, outperforming the state-of-the-art methods. This indicates that our approach can generate urban scene videos that are more consistent with the control conditions.

**Result Analysis of Depth Quality.** In Tab. 1, we report FVD and AbsRel results to evaluate the quality of the generated depth map videos. Compared with the depth maps generated by Depth-Anything-V2, such as CogVideoX + SyntheOcc + Depth-Anything-V2, our approach achieves the better FVD of 25.3 and AbsRel of 0.110. This indicates that the multi-modal generation in our unified framework yields high-quality depth maps, even without using additional models for multi-modal generation.



Methods			RGB	Depth	Semantic
RGB	Depth	Semantic	FVD↓	AbsRel↓	mIoU↑
✓	✗	✗	<b>42.0</b>	0.121	36.4
✓	✓	✗	43.4	0.111	36.0
✓	✓	✓	46.8	<b>0.110</b>	<b>37.5</b>

Table 2. Effectiveness analysis of our multi-modal generation. ‘✓’ means using our approach, ‘✗’ means using the off-the-shelf models.

**Result Analysis of Semantic Quality.** In Tab. 1, we report FVD and mIoU results to evaluate the quality of generated semantic map videos. We can see that our approach achieves better results compared with the state-of-the-art methods, especially in terms of FVD which significantly outperforms the compared methods. This further verifies the effectiveness of our multi-modal generation approach.

### 4.3. Ablation Study

**Effectiveness of Multi-Modal Generation.** In Tab. 2, we analyze the effectiveness of our multi-modal generation mechanism. We compare the performance of ours (RGB) + Depth-Anything-V2 + Mask2Former, ours (RGB + depth) + Mask2Former, and ours (RGB + depth + semantic). From Tab. 2, we can see that our unified approach (RGB + depth + semantic) achieves superior overall performance. Specifically, our approach achieves the best depth AbsRel and semantic mIoU and the comparable RGB FVD. This verifies that generating multiple modalities in a unified framework not only reduces the number of models, but also achieves better overall performance. We visualize some multi-modal generation results in Fig. 5. These results further show the cross-modal consistency of the multi-modal data generated from our approach.

#### Effectiveness of Diffusion Transformer Components.

In Tab. 3, we study the effectiveness of the proposed diffusion transformer model. We can see that using only temporal layer blocks (‘L1’) results in poor performance, while using temporal layer blocks plus modal-specific layer blocks (‘L1+L3’) brings better performance. With all components (‘L1+L2+L3’), our model yields the best performance. Besides, Fig. 6 shows that our approach can maintain cross-view consistency while our approach without using the multi-view spatiotemporal blocks yields poor cross-view consistency.

#### Effectiveness of Unified Layout Condition Encoder.

In Tab. 4, we analyze the effectiveness of our unified layout condition encoder. We can see that using the proposed unified layout condition encoder brings better performance compared with using pre-trained 3D VAE encoders. This can be attributed to the implicit condition embedding

Methods			RGB
L1 blocks	L2 blocks	L3 blocks	FVD↓
✓	✗	✗	153.7
✓	✗	✓	78.8
✓	✓	✓	46.8

Table 3. Effectiveness analysis of the diffusion transformer components. ‘L1’: temporal layers, ‘L2’: multi-view spatiotemporal blocks, ‘L3’: modal-specific layers.

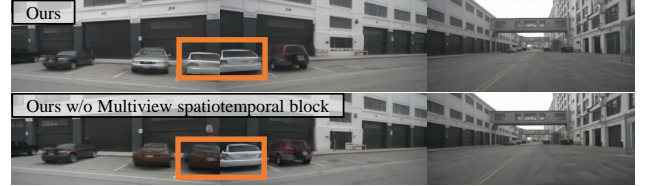


Figure 6. Visualization of cross-view consistency.

Methods	RGB FVD↓
Ours w/ the unified layout condition encoder	46.8
Ours w/o the unified layout condition encoder	53.4

Table 4. Effectiveness analysis of the unified layout condition encoder. ‘w/o the unified layout condition encoder’ means using pre-trained 3D VAE encoders.

space alignment using the proposed module which effectively fuses the conditions for controllable scene generation.

## 5. Conclusion

This work presents a novel multi-modal multi-view urban scene video generation approach to autonomous driving. The key idea is to devise a new multi-modal multi-view diffusion transformer model and leverage diverse conditioning inputs to encode the controllable scene structure and content cues in a unified framework. Extensive experiments on the nuScenes dataset demonstrate the superiority of the proposed approach over the state-of-the-art methods.

**Limitation and Future Work.** While our approach has achieved superior multi-modal multi-view generation performance, there are still limitations. For example, how to effectively combine the proposed approach with a closed-loop autonomous driving simulator is worth further study. This potentially helps to comprehensively evaluate the safety and reliability of autonomous driving systems. In addition, how to derive LiDAR point clouds from the generated multi-modal data is an interesting research direction to further enhance our approach. Our future work aims to explore solutions to these problems to facilitate the deployment of our approach for real-world applications.



## References

- [1] Mohammad Babaeizadeh, Chelsea Finn, Dumitru Erhan, Roy Campbell, and Sergey Levine. Stochastic variational video prediction. In *6th International Conference on Learning Representations, ICLR 2018*, 2018. 2
- [2] Andreas Blattmann, Tim Dockhorn, Sumith Kulal, Daniel Mendelevitch, Maciej Kilian, Dominik Lorenz, Yam Levi, Zion English, Vikram Voleti, Adam Letts, et al. Stable video diffusion: Scaling latent video diffusion models to large datasets. *arXiv preprint arXiv:2311.15127*, 2023. 1, 2
- [3] Holger Caesar, Varun Bankiti, Alex H Lang, Sourabh Vora, Venice Erin Liong, Qiang Xu, Anush Krishnan, Yu Pan, Giancarlo Baldan, and Oscar Beijbom. nuscenes: A multi-modal dataset for autonomous driving. In *Proceedings of the IEEE/CVF conference on computer vision and pattern recognition*, pages 11621–11631, 2020. 2, 5
- [4] Bowen Cheng, Ishan Misra, Alexander G Schwing, Alexander Kirillov, and Rohit Girdhar. Masked-attention mask transformer for universal image segmentation. In *Proceedings of the IEEE/CVF conference on computer vision and pattern recognition*, pages 1290–1299, 2022. 5
- [5] Alexey Dosovitskiy, German Ros, Felipe Codevilla, Antonio Lopez, and Vladlen Koltun. Carla: An open urban driving simulator. In *Conference on robot learning*, pages 1–16. PMLR, 2017. 4
- [6] Ruiyuan Gao, Kai Chen, Bo Xiao, Lanqing Hong, Zhenguo Li, and Qiang Xu. MagicDrive-V2: High-resolution long video generation for autonomous driving with adaptive control. *arXiv preprint arXiv:2411.13807*, 2024. 1, 3, 4, 5, 6
- [7] Ruiyuan Gao, Kai Chen, Enze Xie, HONG Lanqing, Zhenguo Li, Dit-Yan Yeung, and Qiang Xu. Magicdrive: Street view generation with diverse 3d geometry control. In *The Twelfth International Conference on Learning Representations*, 2024. 2, 3, 4, 5, 6
- [8] Shen Yuan Gao, Jiazhi Yang, Li Chen, Kashyap Chitta, Yihang Qiu, Andreas Geiger, Jun Zhang, and Hongyang Li. Vista: A generalizable driving world model with high fidelity and versatile controllability. *arXiv preprint arXiv:2405.17398*, 2024. 3, 7
- [9] Jonathan Ho and Tim Salimans. Classifier-free diffusion guidance. *arXiv preprint arXiv:2207.12598*, 2022. 5
- [10] Jonathan Ho, Ajay Jain, and Pieter Abbeel. Denoising diffusion probabilistic models. *Advances in neural information processing systems*, 33:6840–6851, 2020. 1, 5
- [11] Jonathan Ho, Tim Salimans, Alexey Gritsenko, William Chan, Mohammad Norouzi, and David J Fleet. Video diffusion models. *Advances in Neural Information Processing Systems*, 35:8633–8646, 2022. 2
- [12] Wenyi Hong, Ming Ding, Wendi Zheng, Xinghan Liu, and Jie Tang. Cogvideo: Large-scale pretraining for text-to-video generation via transformers. In *The Eleventh International Conference on Learning Representations*, 2023. 2
- [13] Bohan Li, Jiazhe Guo, Hongsi Liu, Yingshuang Zou, Yikang Ding, Xiwu Chen, Hu Zhu, Feiyang Tan, Chi Zhang, Tiancai Wang, et al. Uniscene: Unified occupancy-centric driving scene generation. In *Proceedings of the Computer Vision and Pattern Recognition Conference*, pages 11971–11981, 2025. 3, 4, 6
- [14] Leheng Li, Weichao Qiu, Yingjie Cai, Xu Yan, Qing Lian, Bingbing Liu, and Ying-Cong Chen. Syntheocc: Synthesize geometric-controlled street view images through 3d semantic mpis. *arXiv preprint arXiv:2410.00337*, 2024. 3, 5, 6, 7
- [15] Xiaofan Li, Yifu Zhang, and Xiaoqing Ye. Drivingdiffusion: Layout-guided multi-view driving scenarios video generation with latent diffusion model. In *European Conference on Computer Vision*, pages 469–485. Springer, 2024. 7
- [16] Zhiqi Li, Wenhai Wang, Hongyang Li, Enze Xie, Chonghao Sima, Tong Lu, Yu Qiao, and Jifeng Dai. Bevformer: Learning bird’s-eye-view representation from multi-camera images via spatiotemporal transformers. In *European Conference on Computer Vision*, pages 1–18, 2022. 6
- [17] Xian Liu, Jian Ren, Aliaksandr Siarohin, Ivan Skorokhodov, Yanyu Li, Dahua Lin, Xihui Liu, Ziwei Liu, and Sergey Tulyakov. Hyperhuman: Hyper-realistic human generation with latent structural diffusion. In *The Twelfth International Conference on Learning Representations*, 2024. 3
- [18] Yibo Liu, Zheyuan Yang, Guile Wu, Yuan Ren, Kejian Lin, Bingbing Liu, Yang Liu, and Jinjun Shan. Vqa-diff: Exploiting vqa and diffusion for zero-shot image-to-3d vehicle asset generation in autonomous driving. In *European Conference on Computer Vision*, pages 323–340. Springer, 2024. 2
- [19] Ben Mildenhall, Pratul P Srinivasan, Matthew Tancik, Jonathan T Barron, Ravi Ramamoorthi, and Ren Ng. Nerf: Representing scenes as neural radiance fields for view synthesis. *Communications of the ACM*, 65(1):99–106, 2021. 3
- [20] Thomas Müller, Alex Evans, Christoph Schied, and Alexander Keller. Instant neural graphics primitives with a multiresolution hash encoding. *ACM transactions on graphics (TOG)*, 41(4):1–15, 2022. 5
- [21] Jingcheng Ni, Yuxin Guo, Yichen Liu, Rui Chen, Lewei Lu, and Zehuan Wu. Maskgwm: A generalizable driving world model with video mask reconstruction. In *Proceedings of the Computer Vision and Pattern Recognition Conference*, pages 22381–22391, 2025. 1, 3, 4, 6
- [22] Colin Raffel, Noam Shazeer, Adam Roberts, Katherine Lee, Sharan Narang, Michael Matena, Yanqi Zhou, Wei Li, and Peter J Liu. Exploring the limits of transfer learning with a unified text-to-text transformer. *Journal of machine learning research*, 21(140):1–67, 2020. 3, 6
- [23] Yuan Ren, Guile Wu, Runhao Li, Zheyuan Yang, Yibo Liu, Xingxin Chen, Tongtong Cao, and Bingbing Liu. Unigaussian: Driving scene reconstruction from multiple camera models via unified gaussian representations. *arXiv preprint arXiv:2411.15355*, 2024. 2
- [24] Robin Rombach, Andreas Blattmann, Dominik Lorenz, Patrick Esser, and Björn Ommer. High-resolution image synthesis with latent diffusion models. In *Proceedings of the IEEE/CVF conference on computer vision and pattern recognition*, pages 10684–10695, 2022. 1
- [25] Jiaming Song, Chenlin Meng, and Stefano Ermon. Denoising diffusion implicit models. In *International Conference on Learning Representations*, 2021. 5

- [26] Gabriela Ben Melech Stan, Diana Wofk, Scottie Fox, Alex Redden, Will Saxton, Jean Yu, Estelle Aflalo, Shao-Yen Tseng, Fabio Nonato, Matthias Muller, et al. Ldm3d: Latent diffusion model for 3d. *arXiv preprint arXiv:2305.10853*, 2023. 3
- [27] Sergey Tulyakov, Ming-Yu Liu, Xiaodong Yang, and Jan Kautz. Mocogan: Decomposing motion and content for video generation. In *Proceedings of the IEEE conference on computer vision and pattern recognition*, pages 1526–1535, 2018. 2
- [28] Thomas Unterthiner, Sjoerd Van Steenkiste, Karol Kurach, Raphael Marinier, Marcin Michalski, and Sylvain Gelly. Towards accurate generative models of video: A new metric & challenges. *arXiv preprint arXiv:1812.01717*, 2018. 6
- [29] Xiaofeng Wang, Zheng Zhu, Guan Huang, Xinze Chen, Jia-gang Zhu, and Jiwen Lu. Drivedreamer: Towards real-world-drive world models for autonomous driving. In *European Conference on Computer Vision*, pages 55–72. Springer, 2024. 1, 2, 3, 4, 5, 6
- [30] Yuqi Wang, Ke Cheng, Jiawei He, Qitai Wang, Hengchen Dai, Yuntao Chen, Fei Xia, and Zhao-Xiang Zhang. Driving-dojo dataset: Advancing interactive and knowledge-enriched driving world model. *Advances in Neural Information Processing Systems*, 37:13020–13034, 2024. 3
- [31] Yuqi Wang, Jiawei He, Lue Fan, Hongxin Li, Yuntao Chen, and Zhaoxiang Zhang. Driving into the future: Multiview visual forecasting and planning with world model for autonomous driving. In *Proceedings of the IEEE/CVF Conference on Computer Vision and Pattern Recognition*, pages 14749–14759, 2024. 3, 6
- [32] Dirk Weissenborn, Oscar Täckström, and Jakob Uszkor-eit. Scaling autoregressive video models. *arXiv preprint arXiv:1906.02634*, 2019. 2
- [33] Yuqing Wen, Yucheng Zhao, Yingfei Liu, Fan Jia, Yanhui Wang, Chong Luo, Chi Zhang, Tiancai Wang, Xiaoyan Sun, and Xiangyu Zhang. Panacea: Panoramic and controllable video generation for autonomous driving. In *Proceedings of the IEEE/CVF Conference on Computer Vision and Pattern Recognition*, pages 6902–6912, 2024. 1, 3, 6
- [34] Guile Wu, Dongfeng Bai, and Bingbing Liu. Ar-mgs: Composite gaussian appearance refinement for modeling dynamic urban environments. *arXiv preprint arXiv:2507.03886*, 2025. 2
- [35] Dianbing Xi, Jiepeng Wang, Yuanzhi Liang, Xi Qiu, Yuchi Huo, Rui Wang, Chi Zhang, and Xuelong Li. Omnivdiff: Omni controllable video diffusion for generation and understanding. *arXiv preprint arXiv:2504.10825*, 2025. 3
- [36] Lihe Yang, Bingyi Kang, Zilong Huang, Zhen Zhao, Xiaogang Xu, Jiashi Feng, and Hengshuang Zhao. Depth anything v2. *Advances in Neural Information Processing Systems*, 37:21875–21911, 2024. 5, 6
- [37] Ze Yang, Yun Chen, Jingkan Wang, Sivabalan Manivasagam, Wei-Chiu Ma, Anqi Joyce Yang, and Raquel Urtasun. Unisim: A neural closed-loop sensor simulator. In *Proceedings of the IEEE/CVF Conference on Computer Vision and Pattern Recognition*, pages 1389–1399, 2023. 2
- [38] Zhuoyi Yang, Jiayan Teng, Wendi Zheng, Ming Ding, Shiyu Huang, Jiazheng Xu, Yuanming Yang, Wenyi Hong, Xiaohan Zhang, Guanyu Feng, et al. Cogvideox: Text-to-video diffusion models with an expert transformer. In *The Thirteenth International Conference on Learning Representations*, 2025. 1, 2, 4, 5, 6, 7
- [39] Yuanhao Zhai, Kevin Lin, Linjie Li, Chung-Ching Lin, Jianfeng Wang, Zhengyuan Yang, David Doermann, Junsong Yuan, Zicheng Liu, and Lijuan Wang. Idol: Unified dual-modal latent diffusion for human-centric joint video-depth generation. In *European Conference on Computer Vision*, pages 134–152. Springer, 2024. 3
- [40] Guosheng Zhao, Xiaofeng Wang, Zheng Zhu, Xinze Chen, Guan Huang, Xiaoyi Bao, and Xingang Wang. Drivedreamer-2: Llm-enhanced world models for diverse driving video generation. In *Proceedings of the AAAI Conference on Artificial Intelligence*, pages 10412–10420, 2025. 4, 6
- [41] Hongyu Zhou, Jiahao Shao, Lu Xu, Dongfeng Bai, Weichao Qiu, Bingbing Liu, Yue Wang, Andreas Geiger, and Yiyi Liao. Hugs: Holistic urban 3d scene understanding via gaussian splatting. In *Proceedings of the IEEE/CVF Conference on Computer Vision and Pattern Recognition*, pages 21336–21345, 2024. 2